Nuclear Science and Techniques (2023) 34:179
https://doi.org/10.1007/s41365-023-01335-8

PSA study of the effect of extreme snowfall on a floating nuclear power plant: case study in the Bohai Sea

Lan-Xin Gong[1] · Qing-Zhu Liang[1] · Chang-Hong Peng[1]

Received: 22 May 2023 / Revised: 28 June 2023 / Accepted: 18 July 2023 / Published online: 22 November 2023

Abstract
This study presents a probabilistic safety analysis (PSA) method for the external event of extreme snowfall on a floating nuclear power plant (FNPP) deployed in the Bohai Sea. We utilized the Weibull and Gumbel extreme value distributions to fit the collected meteorological data and obtained a hazard curve for the event of an extreme snowfall where the FNPP is located, providing a basis for the frequency of extreme snowfall-initiating events. Our analysis indicates that extreme snowfall primarily affects the ventilation openings of the equipment, leading to the failure of devices such as the diesel generators. Additionally, extreme snowfall can result in a loss of off-site power (LOOP). Therefore, the developed extreme snowfall PSA model is mainly based on the LOOP event tree, considering responses such as snowfall removal by personnel. Our calculations indicate a core damage frequency (CDF) of 1.13×10^{-10} owing to extreme snowfall, which is relatively low. The results of the cut-set analysis indicate that valve failures in the core makeup tank (CMT), passive residual heat removal system (PRS), and in-containment refueling water storage tank (IRWST) significantly contribute to the CDF.

Keywords Floating nuclear power plant (FNPP) · ACP100 · Extreme snow PSA · External hazard

1 Introduction

Floating nuclear power plants (FNPPs) have recently gained increasing attention owing to their flexible deployment and ability to provide heat, electricity, and water cogeneration for remote islands/regions [1–3]. To meet the needs of offshore platforms, an integrated pressurized water reactor (IPWR) that is compact, small, and has muscular mobility is usually selected as the FNPP, such as the ACP100 (Advanced China Power 100). As a small modular reactor (SMR), the safety system of ACP100 adopts a passive design concept to achieve reactor safety under accidents owing to natural forces, which reduces the dependence on external water sources, power supplies, and personnel intervention. The following key engineered passive safety systems are included: core cooling, residual heat removal, and containment air cooling. The design system follows a single-failure principle, and no human intervention is required 72 h after an accident [2, 4]. A potential deployment site was selected in Yantai in the Bohai region. Prior to formal testing, a probabilistic safety analysis (PSA) of an FNPP is crucial for project development.

Owing to the currently limited deployment of FNPPs, studies regarding their safety have mainly focused on deterministic analyses, including thermal-hydraulic characteristics [5], structural stresses [6], and severe accident analyses [7]. Studies regarding probabilistic analyses, especially those concerning external events, are limited, with current research primarily focusing on ship collisions [8]. According to meteorological data, heavy snowfall occurred in Yantai, where the FNPP was deployed. Considering the integrity of the safety assessment, it is necessary to consider the impact of extreme snowfall on an FNPP. In addition, incorporating extreme snowfall as an external event into the probabilistic safety assessment will have potential benefits for the design of an FNPP and the identification of risks for other nuclear power plants along the Bohai coast. This study aims to evaluate the impact of extreme snowfall on an FNPP using meteorological data within the framework of a risk assessment of an external event and to provide risk insights for the design of an FNPP.

✉ Chang-Hong Peng
pengch@ustc.edu.cn

[1] School of Nuclear Science and Technology, University of Science and Technology of China, Hefei 230026, China

Experts have typically used the general analysis framework of an external event [9] extracted from the earthquake PSA and strong-wind PSA to analyze extreme snowfall. The framework typically includes the following several elements: (1) the use of specific criteria for disaster screening to eliminate extremely unlikely hazards or combinations thereof, (2) using the collected data, selecting appropriate hazard intensity measures, and conducting disaster risk analyses to obtain the frequency of the initiating events (IEs), and (3) establishing a quantitative model of the impact of a hazard, typically an event tree (ET) or fault tree (FT) model.

Researchers have studied both light water reactors (LWRs) and non-LWRs within this framework. The screening of hazards is based on a series of standards, including the ASME/ANS Standards [10, 11], IAEA NS-R-3 [12], and IAEA SSG-3 [13], which are summarized in technical reports [14]. Narumiya et al. [15] proposed a method for selecting combined hazards by calculating risk factors (product of the frequency and consequences). Choi et al. [16] discussed the classification, combination, and impact of external hazards on nuclear power plants (NPPs) and provided risk calculations (multidimensional integrals) for specific combinations. Kubo et al. [17] established a method to quantify the risks caused by multiple combinations of hazards. Considering the correlation between earthquakes and flood failures, they conducted a dynamic probabilistic risk assessment (PRA) of earthquake-induced flood events. In addition, they were coupled with a thermal hydraulics code and risk assessment using a plant interactive dynamics (RAPID) framework. Yamano et al. [18] developed a PRA method for the combined hazards of strong winds and heavy rain. The combined analysis of the risk probability evaluates the risk curve based on the maximum instantaneous wind speed, hourly rainfall, and duration. Kantarzhi et al. [19] developed an ice dynamics model for the Russian FNPP deployment environment. Based on meteorological data and site conditions, they determined the ice loads on the structure of the FNPP.

Considering the PSA of extreme snowfalls, scholars typically use the depth of snow [9],maximum load of the frost and icing [9], snow rate [20], low-temperature duration [21], minimum temperature [22], blockage [23], or a combination of the hazard intensities. Juraj [24] utilized ANSYS to study the load effects of extreme snowfall with a return period of 10^4 years on structures. Scholars typically use extreme value distributions (including the Gumbel and Weibull distributions) to describe the distribution of hazard quantities for disaster risk analyses.

The PSA models for snow are typically developed based on a Level 1 PSA. By analyzing the impact of extreme snowfall on the SSCs, the PSA model of an internal event can be added to the snow PSA. The Japan Atomic Energy Agency (JAEA) developed sodium fast reactors (SFRs) and conducted a PSA under a combination of extreme snowfall and low temperatures. Yamano et al. [21, 25] converted 50-year weather data from a typical SFR plant site into hazard intensities (annual maximum snow depth and annual maximum snow depth) and obtained the relevant hazard curve. The results demonstrate that the vital action of humans is critical for improving the speed of snow removal and achieve the necessary snow removal. Assuming that the initiating event is a loss of off-site power, Nishino et al. [20] also considered recovery measures to prevent the loss of DHRS functionality (snow removal and filter replacement) and installed electric heaters around the inlet and outlet as an additional countermeasure.

Because the deployment area of an FNPP can be offshore or in the open sea, both mobile and moored deployments pose a challenge in collecting meteorological data for snow hazards. The FNPP investigated in this study is expected to be deployed offshore of Yantai and is not intended to move widely [3]. Therefore, utilizing the meteorological data of nearby land to characterize the deployment site is acceptable.

As indicated in the aforementioned, the scope of the PSA in this study will be limited to Level 1. Similar to the analysis framework of land-based nuclear power plants [26, 27], the Level 1 PSA of FNPP usually includes initiating events, event sequences, success criteria, and human factor analysis. Considering the difference between the external and internal PSAs for an FNPP in the event of an extreme snowfall, the external initiating events were mainly focused on. The entire analysis ultimately estimates the core damage frequency (CDF) and helps understand the advantages and disadvantages of existing or envisaged safety-related systems and procedures for preventing core damage.

2 Extreme snowfall hazard analysis

2.1 Methodology

Establishing a PSA model for external events cannot be separated from hazard analysis. The analysis of an extreme snow hazard aims to determine the intensity and frequency of the hazards. The intensity of extreme snowfall can be characterized by the thickness of the snow or rate of snowfall. The results of the extreme snowfall risk analysis typically include the annual exceedance probability of the snow thickness, snowfall rate, or a combination of the two [20, 21]. By collecting and processing the snow-related data of Yantai, the extreme value distribution can be used to fit the annual exceedance probability of the snow thickness or snowfall rate, including the Type I extreme value distribution (Gumbel distribution) and type III extreme value distribution (Weibull distribution) [21, 28, 29]. The cumulative distribution function formulas are as follows:

$$F(X) = \exp\left\{-\exp\left[-\left(\frac{X-\mu}{\theta}\right)\right]\right\}, \tag{1}$$

$$F(X) = 1 - \exp\left[-\left(\frac{X}{\eta}\right)^m\right], \tag{2}$$

where X is the snow depth (cm) or snowfall speed (cm/day), m is the shape parameter of the Weibull distribution, θ is the scale parameter of the Gumbel distribution, η is the scale parameter of the Weibull distribution, and μ is the location parameter of the Gumbel distribution.

Assuming that the sample data of the maximum annual snow depth or snowfall speed of the plant site for N consecutive N years are collected and sorted as x_i $(i = 1, 2, .., N)$ from small to large, the cumulative probability of x_i of the i–th maximum can be estimated according to the Cunnane criterion as follows:

$$F(x_i) = \frac{i-\alpha}{N+1-2\alpha} \tag{3}$$

where N is the total number of data points and α is the coefficient of the plotting position formula. The coefficients of the plotting position formula α are $\alpha = 0$ for the Weibull, $\alpha = 1/2$ for Hazen and $\alpha = 2/5$ for Cunnane distributions. According to Yamano [21], we assume that $\alpha = 2/5$.

The appropriate transformations of Eqs. 1 and 2, as shown in Eqs. 4 and 5, can be used to estimate the parameters of the Gumbel and Weibull distributions using least-squares linear fitting methods, as shown in Eqs. 6 and 8.

$$-\ln\{-\ln[F(X)]\} = \frac{1}{\theta}X - \frac{\mu}{\theta} \tag{4}$$

$$\ln\{-\ln[1-F(X)]\} = m\ln X - m\ln\eta \tag{5}$$

$$\frac{1}{\theta} = \frac{\sum_{i=1}^{m}\left(x_i-\bar{x}\right)\left\{-\ln\left\{-\ln\left[F\left(x_i\right)\right]\right\}-\bar{y}\right\}}{\sum_{i=1}^{m}\left(x_i-\bar{x}\right)^2} \tag{6}$$

$$\frac{\mu}{\theta} = \bar{y} - \frac{1}{\theta}\bar{x} \tag{7}$$

where

$$\bar{x} = \frac{\sum_{i=1}^{m} x_i}{m}, \bar{y} = \frac{\sum_{i=1}^{m} -\ln\left\{-\ln\left[F\left(x_i\right)\right]\right\}}{m}$$

$$m = \frac{\sum_{i=1}^{m}\left(\ln x_i-\bar{x}\right)\left\{\ln\left\{-\ln\left[1-F\left(x_i\right)\right]\right\}-\bar{y}\right\}}{\sum_{i=1}^{m}\left(\ln x_i-\bar{x}\right)^2} \tag{8}$$

$$m\ln\eta = \bar{y} - m\bar{x} \tag{9}$$

where $\bar{x} = \frac{\sum_{i=1}^{m}\ln x_i}{m}, \bar{y} = \frac{\sum_{i=1}^{m}\ln\left\{-\ln\left[1-F\left(x_i\right)\right]\right\}}{m}$.

Thus far, we can estimate the extreme value distribution of the meteorological data. We used the K-S test to determine whether the distribution estimation was appropriate. Given the cumulative distribution function $F_0(x)$ of the hypothesized distribution and the empirical distribution function $F_{\text{data}}(x)$ of the observed data, the test statistic is given by the following:

$$D = \sup_x \left|F_0(x) - F_{\text{data}}(x)\right| \tag{10}$$

For the non-decreasing functions f and g, the estimate of Eq. 10 can be calculated as follows [30]:

$$\sup_x |f(x)-g(x)| = \max_i\left[\max\left(\left|g\left(x_i\right)-f\left(x_i\right)\right|, \lim_{x\to x_i}\left|g(x)-f\left(x_{i-1}\right)\right|\right)\right] \tag{11}$$

$$= \max_i\left[\max\left(\left|g\left(x_i\right)-f\left(x_i\right)\right|, \left|g\left(x_i\right)-f\left(x_{i-1}\right)\right|\right)\right] \tag{12}$$

$$= \max\left[\max_i\left|g(x_i)-f(x_i)\right|, \max_i\left|g(x_i)-f(x_{i-1})\right|\right] \tag{13}$$

where sup indicates the supremum. Further details can be found in Appendix A.

2.2 Case study in the Bohai Sea

2.2.1 Collection of historical records

The FNPP off Yantai was considered as the research object, and a case study for the risk analysis of extreme snowfall was provided. Owing to the lack of data regarding the snow thickness in Yantai, we obtained the daily temperatures (maximum, minimum, and average) and precipitation data over the past 39 years from the National Greenhouse Data System [31] and the National Centers for Environmental Information (NCEI) [32]. The two meteorological stations (Yantai and Yantai North) that were nearest to the FNPP were adopted.

According to the definitions provided by the China Meteorological Administration, the formation of snow occurs by the direct sublimation of water vapor in the atmosphere or the direct solidification of water droplets. Specifically, the conditions for the formation of snowfall are as follows: (1) the presence of ice crystals in the atmosphere, (2) sufficient water vapor, and (3) an air temperature below 3 °C (freezing point). Based on the aforementioned conditions, an average temperature of less than 3 °C along with the occurrence of precipitation on a particular day is considered snowfall. Because the staff of a nuclear power plant can usually clear snow within 24 h, the snowfall was analyzed for a limited duration of one day. The snow-to-liquid ratio (SLR) refers to the ratio of the depth of snow to the equivalent depth of the liquid after the snow melts, which can be used to calculate the snow depth.

$$SLR = \frac{SD}{SL} \tag{14}$$

Here, SLR indicates the snow-to-liquid ratio (cm/mm), SD denotes the new accumulated snow depth (cm) between the current and following day, and SL indicates the accumulated precipitation (mm) within the same period as that of the new snow depth.

Yang et al. [33] demonstrated that the multiyear average SLR in the northern coastal area of the Shandong Peninsula (in the Bohai Sea), which is known for ocean-effect snowstorms, was 1.3 cm/mm. The distribution of SLR in the northern Shandong Peninsula, including Yantai, is approximately a normal distribution, with a mean value of 1.30 and a variance of 0.65. Considering the significant uncertainties in the meteorological data, we also studied their impact on the hazard curve, as shown in Table 1. Based on the SLR, precipitation was converted into snow depth and sorted, as indicated in Table 2. Subsequently, the snowfall rate was calculated using Eq. 15 based on the calculated snow depth SD and duration of snowfall ΔT; it was also sorted and is included in Table 2.

$$SV = \frac{SD}{\Delta T} \tag{15}$$

2.2.2 Annual exceedance probability evaluation

Using the analysis method described in Sect. 2.1, the Gumbel and Weibull distributions were used to fit the snow depth and speed of the extreme snowfall. The results are presented in Table 3, and a comparison between the fitted value of the cumulative probability and measured value is shown in Figs. 1 and 2. As shown in Fig. 2, the deviation between the Gumbel fitting value and the measured value was within 20% for snow thickness. The deviation between the fitted and measured values was significant for the small measured values, whereas it was within 20% for the significant measured values. For the snowfall rate, the deviation between the fitted values of the two distributions and the measured value was relatively large. The deviation between the measured values was within the range of 20%. These findings

Table 2 Extreme snowfall data of Yantai. SLR=1.3 cm/mm

No	Cumulative distribution function	Snow depth (cm)	Snow speed (cm/day)
1	0.015306	2.60	1.72
2	0.040816	2.99	1.85
3	0.066327	4.42	1.91
4	0.091837	4.55	2.60
5	0.117347	4.55	2.77
6	0.142857	5.20	2.99
7	0.168367	5.72	3.02
8	0.193878	5.98	3.06
9	0.219388	6.89	3.42
10	0.244898	8.32	3.64
11	0.270408	9.23	3.66
12	0.295918	10.79	4.10
13	0.321429	11.31	4.42
14	0.346939	11.96	4.55
15	0.372449	12.09	4.55
16	0.397959	12.09	5.20
17	0.423469	12.22	5.33
18	0.448980	13.845	5.40
19	0.474490	14.56	5.66
20	0.500000	16.185	5.98
21	0.525510	16.38	6.05
22	0.551020	17.615	6.92
23	0.576531	17.94	7.93
24	0.602041	18.07	8.97
25	0.627551	18.72	9.04
26	0.653061	19.695	9.36
27	0.678571	20.54	9.36
28	0.704082	20.605	9.36
29	0.729592	21.06	10.30
30	0.755102	21.71	10.79
31	0.780612	23.79	10.86
32	0.806122	25.61	11.96
33	0.831633	27.495	13.75
34	0.857143	28.08	17.62
35	0.882653	31.98	19.70
36	0.908163	37.44	19.89
37	0.933673	52.39	21.06
38	0.959184	59.67	26.20
39	0.984694	84.24	84.24

Table 1 Uncertainty parameter of SLR, unit: cm/mm

Type	Value
Minimum	0.7
25th percentile value	1.2
Median	1.3
75th percentile value	1.6
Maximum	2.0

Table 3 Fitting results of the extreme snow hazard (SLR = 1.3 cm/mm), parameters: μ, θ or η, m. The confidence boundary for the parameter uncertainty is 95%

Distribution	Parameters	Parameters Uncertainty	p value
Snow depth			
Gumbel	(11.85, 9.12)	(11.54, 12.15), (8.65, 9.59)	0.9926
Weibull	(19.05, 1.58)	(18.63, 19.47), (1.49, 1.67)	0.9843
Snow speed			
Gumbel	(5.14, 4.27)	(4.90, 5.38), (3.87, 4.68)	0.7144
Weibull	(8.63, 1.42)	(8.28, 8.98), (1.31, 1.54)	0.8305

Table 4 The uncertainty of the distribution of the fitting parameters, considering the SLR uncertainty and fitting uncertainty. The confidence boundary for the parameter uncertainty is 95%

Snow speed parameter	η	m
Value	(5.2203, 12.7134)	(1.4207, 1.4209)
Snow depth parameter	μ	θ
Value	(7.1643, 17.4485)	(5.5178, 13.4383)

are consistent with those in other studies [21]. Based on the analysis results, it is recommended to use the Gumbel distribution to fit the annual exceedance probability of the snow thickness, and the Weibull distribution to fit the snow rate, for the hazard analysis of extreme snow of the Yantai plant site.

There are two primary sources of uncertainty regarding the snow speed and depth. The first source of uncertainty is the original meteorological data, which refers to the SLR uncertainty discussed in this study. We use the minimum (SLR = 0.7 cm/mm) and maximum values (SLR = 1.3 cm/mm) in the hazard curve to represent the uncertainty, as depicted in Fig. 3. We provided the 5th (SLR = 0.786 cm/mm) and 95th (SLR = 1.914 cm/mm) percentile values of the SLR to quantify the uncertainty. Another source of uncertainty is the parameter uncertainty inherent in the fitting distribution process. Table 3 lists the uncertainties encountered during the fitting process for a given SLR. Table 4 presents the 95th percentile results for the two types of parameters under uncertainty.

2.2.3 Snow hazard curves and evaluation

Annual exceedance frequency refers to the probability of a specific event or phenomenon occurring within a given year. It represents the likelihood of an event surpassing a certain threshold or level within a single year. Typically, the annual exceedance frequency of external events is used as the frequency of initiating events. The annual exceedance probability ($1 - F(x)$) curves of the snow depth and snowfall speed are shown in Fig. 3. The solid line represents the fitted hazard curve obtained by applying the corresponding distribution function to the data points. To consider the uncertainty of the SLR, we plotted the hazard curves under the conditions of the maximum, minimum, and median SLR, as shown in Fig. 3. This demonstrates that the uncertainty of the hazard analysis results caused by the uncertainty of the SLR can reach several orders of magnitude for significant hazard parameters (snow depth, snow speed).

3 Power plant response and the impact of extreme snowfall on safety-related SSCs

The impacts of extreme snowfall on floating nuclear power plants include the following: direct damage of snow load on buildings, snow blockage of ventilation holes, and the indirect impact of long-term power plant isolation. The potential damage from extreme snowfall significantly varies owing to the characteristics of snow. The specific impacts of extreme snowfall on an FNPP are as follows:

- Damage of structure and exposed parts caused by snow load.
- The failure of systems and equipment that depend on air circulation owing to the blockage of snow at the vent, mainly the heating, ventilation and air conditioning (HVAC) system and diesel generator equipment.
- Loss of off-site power (LOOP).

All buildings, regardless of the safety classification, are designed to withstand the impact of snow. In addition, the design of safety-grade buildings can prevent aircraft crashes, earthquakes, and external hazards, thereby providing sufficient safety margins against extreme snowfall. Juraj et al. [24] also confirmed this, demonstrating that structures have a failure load that is nearly twice the magnitude of extreme snow loads. Therefore, the main impact of extreme snowfall on floating nuclear power plants is possibly the failure of systems and equipment that depend on air circulation owing to the blockage of snow at the vent and loss of off-site power caused by extreme snowfall. Whether an FNPP requires off-site power depends on its design. Because the FNPP in our study is located offshore, off-site power can be supplied through submarine cables. Although the impact of extreme snowfall on submarine cables is lower than its impact on off-site power for onshore NPPs, considering that onshore power transmission and conversion equipment are located in the same area as the FNPP, this study assumes that a snowfall thickness exceeding 100 cm causes damage to the off-site power grid equipment, leading to LOOP.

Fig. 1 Distribution fitting of the snowfall extreme value data ▶ (SLR=1.3 cm/mm)

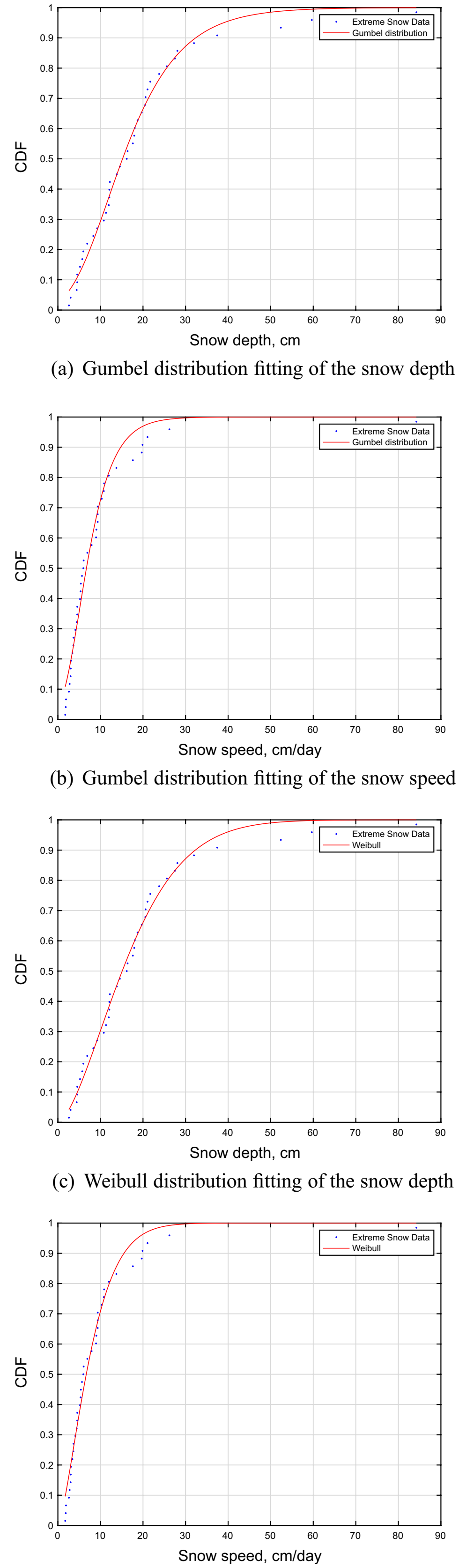

(a) Gumbel distribution fitting of the snow depth

(b) Gumbel distribution fitting of the snow speed

(c) Weibull distribution fitting of the snow depth

(d) Weibull distribution fitting of the snow speed

In our study, the extreme snowfall led to a LOOP-initiating event. When a LOOP occurs in a land-based nuclear power plant, the dependency of the safety-related systems on the electrical power system can impact the accident sequence. In particular, equipment failures during a LOOP event, such as valves being unable to open or close, may result in the inability to perform the corresponding safety functions, leading to an inability to lower the reactor pressure and cool the core [34]. This situation is similar for an FNPP. The response of the safety-related system equipment of the plant resembles its response to an internal LOOP event, and an on-site emergency power supply must be considered. A combination of the successful or failed responses of the residual heat removal, pressure relief, and safety injection functions were utilized for the event sequence analysis. It is also possible to consider snow clearing at the vent in response to extreme snowfall events at a power plant. In this case, if the relevant personnel do not recognize the necessity of clearing snow, the snow at the vent will reach a threshold, and blockage of the vent may lead to the unavailability of the diesel generator. It is conservatively assumed that the unavailability of the diesel generators will lead to a loss of the emergency power supply of the plant, leading to a secondary station blackout (SBO) accident. Subsequently, the response process of the power plant must consider the loss of the relevant system that supports the power supply. The diesel generator is the main equipment affected by snow blockages at the vent. Although snow blockage at the vent may also lead to the failure of the HVAC systems, resulting in a gradual rise in the temperature within the plant, it may also lead to the failure of the diesel generator, which is a slow development process that can be included in the previous impact.

4 Extreme snowfall PSA model

The event tree (ET) analysis describes the response of a power plant to the initiating events through a series of events, linking the success or failure of several safety systems/functions to the final states of the plant (intact core: OK/core damage: CD). Based on previous assumptions, extreme snowfall events lead to the loss of the off-site power supply (LOOP) of floating nuclear power plants. Based on the Level 1 PSA model of an internal event [4] of an FNPP, an event tree model of extreme snowfall events for an FNPP was developed by referring to the event tree of the LOOP of an internal event and considering the unique snow removal response of extreme snowfall events. An event tree model of the core damage caused by extreme snowfall in an FNPP

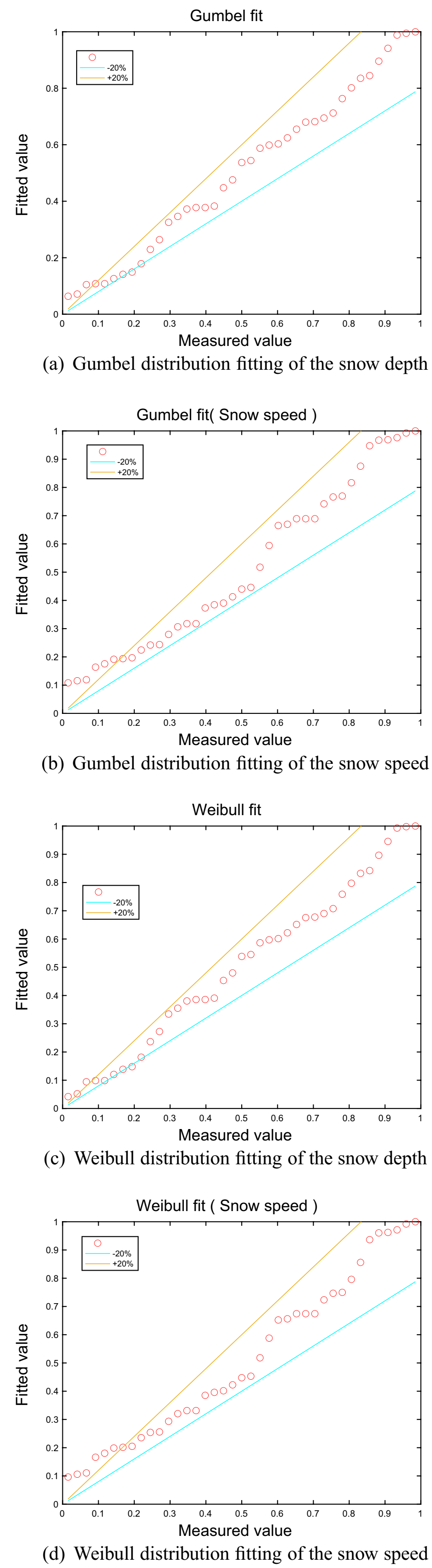

(a) Gumbel distribution fitting of the snow depth

(b) Gumbel distribution fitting of the snow speed

(c) Weibull distribution fitting of the snow depth

(d) Weibull distribution fitting of the snow speed

Fig. 2 Cumulative probability measurement and fitting values ▶ (*SLR*=1.3 cm/mm)

can be developed by combining the system model of a Level 1 PSA model of an internal event with personnel reliability modeling. The event trees in the PSA model are shown in Fig. 4 through Fig. 7. The abbreviations of the function events in the event trees are listed in Table 5 (Figs. 5, 6).

A fault tree (FT) analysis is a standard method for the reliability assessment in nuclear power plants, enabling the determination of the probabilities of the top events in event trees. It utilizes graphical and top-down approaches to decompose complex system failures from the system to the component level. Based on the design of various safety-related systems in ACP100 [35] and by referring to the fault tree of AP1000, we established fault trees for the safety systems of the FNPP. Figures 8 and 9 present the corresponding fault trees for the DGEN and PRS functional events. In the FNPP PSA model, the FT method is also employed for a system reliability analysis [36], considering factors such as random failures, common-cause failures (CCF) of equipment, human errors, unavailability owing to testing and maintenance, and failures in support systems. The Multiple Greek Letter (MGL) model was adopted for the CCF analysis in the PSA software called Risk Spectrum. Regarding human errors, the primary consideration is the impact of personnel unreliability on equipment during the initiation of events. The data are primarily obtained from NUREG/CR-1278 [37], and an example of the snow clearance by personnel affecting the on-site power is discussed in this section. The model parameters and logic for equipment testing and maintenance were set accordingly in Risk Spectrum, with data primarily sourced from AP1000, ACP100, and NUREG/CR-6928 [38].

The data required to quantify the CDF caused by extreme snowfall in floating nuclear power plants include the relevant data used in the Level 1 PSA model of an internal event, the frequency of LOOP-initiating events caused by the extreme snowfall, and the probability of snow removal failure. The frequency of LOOP-initiating events caused by extreme snowfall can be estimated based on a site-specific risk analysis of extreme snowfall. As shown in Table 6, we analyzed the annual exceedance frequency corresponding to a snow depth of 100 cm and snowfall speed of 100 cm/day and finally obtained the most conservative result (3.00×10^{-3}/plant year) as the frequency of the initial event.

According to Noroozi et al. [39], the impacting factors of extreme snowfall on the workers include low temperatures, freezing, comprehensive weather effects, ocean ice, low visibility, and work pressures. According to Islam et al. [40], the impact is mainly owing to the following several aspects: (1) Compared to land-based nuclear power plants, floating platform environments can generate ship motion, noise, and

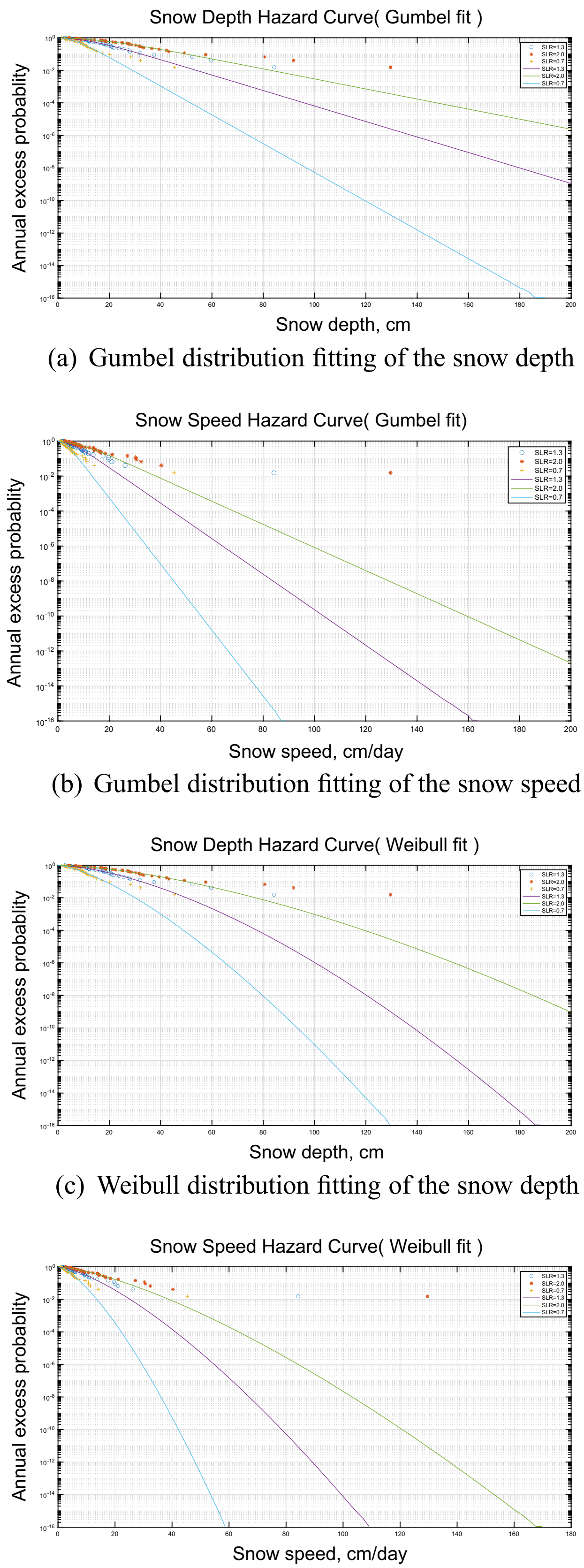

(a) Gumbel distribution fitting of the snow depth

(b) Gumbel distribution fitting of the snow speed

(c) Weibull distribution fitting of the snow depth

(d) Weibull distribution fitting of the snow speed

Fig. 3 Hazard curve of the snowfall

Table 5 Abbreviations in event trees

Abbreviation	Full form
CMT	Core makeup tank
CSP	Containment spray
DGEN	LOOP and power source not recovered after 30 min
DHRS	Decay heat removal system
EDG	Emergency diesel generator
LOCA	Loss of coolant accident
LOFW	Loss of feed-water
LOOP	Loss of off-site power
LPI	Low pressure safety injection
LPI-C	Low pressure safety injection recirculation
MLOCA	Medium break LOCA
PRS	Passive residual heat removal system
PZRSVC	Pressurizer safety valve fail to close
PZRSVO	Pressurizer safety valve fail to open
RHR	Residual heat removal system
SWR	Snow remove
SNOW	Extreme snowfall

vibration under extreme snowfall, which increases the workload and pressure of snow-clearing personnel. (2) Low ambient temperatures may lower the body temperature, severely affecting the mental and sensory abilities and making it difficult to accurately determine the blockage locations. (3) Cold weather can significantly reduce physical performance and hinder the completion of snow-clearing tasks.

A simple reliability model considering the following two aspects can be adopted for snow removal at the air vent: (1) reliability of the relevant personnel realizing the necessity of snow removal, P_{AW}; (2) reliability of the snow removal operation, P_{RM}. The probabilities of failure of the two aforementioned types of events can be evaluated using an appropriate probability of human error, as expressed in Eq. 16. Based on the data above, the CDF caused by the extreme snowfall of a specific floating nuclear power plant can be estimated to assess the risk of floating nuclear power plants caused by extreme snowfall.

$$P_{\text{SW-RM}} = P_{\text{AW}} + P_{\text{RM}} = 7.35 \times 10^{-3} \tag{16}$$

Here, the values indicated in the formula above can be found in NUREG/CR-1278 [37]. Although the values of NUREG/CR-1278 are typically used in land-based nuclear power plants, this result is acceptable considering the similarity between land-based nuclear power plants and FNPPs, as well as the conservatism of the probability of failure in NUREG/CR-1278.

The probability of failure of an individual receiving good skills training for 60 min to perform the step-by-step task under the average pressure level was used to estimate P_{AW}

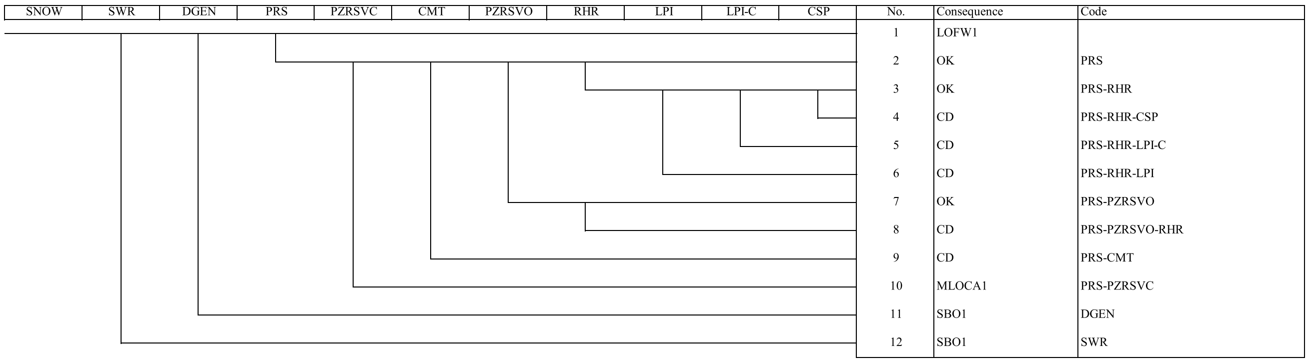

Fig. 4 FNPP event tree (initial event: extreme snowfall)

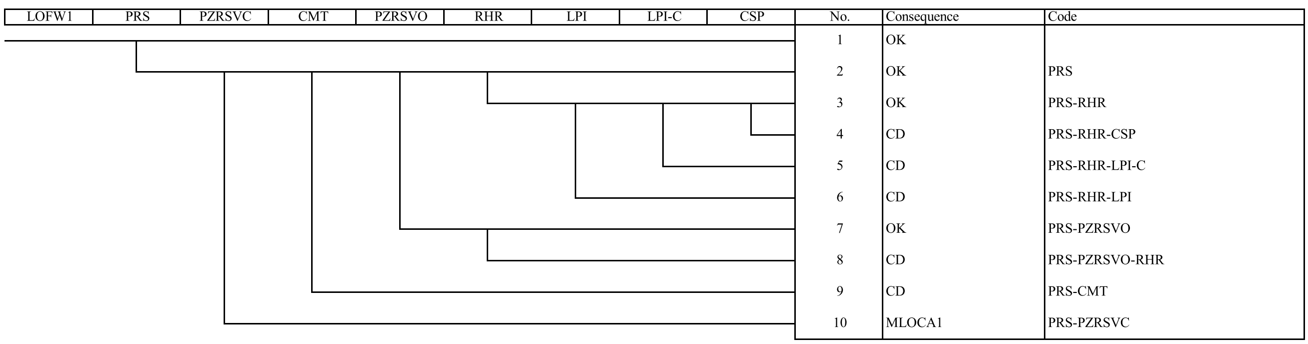

Fig. 5 FNPP event tree (secondary event: LOFW)

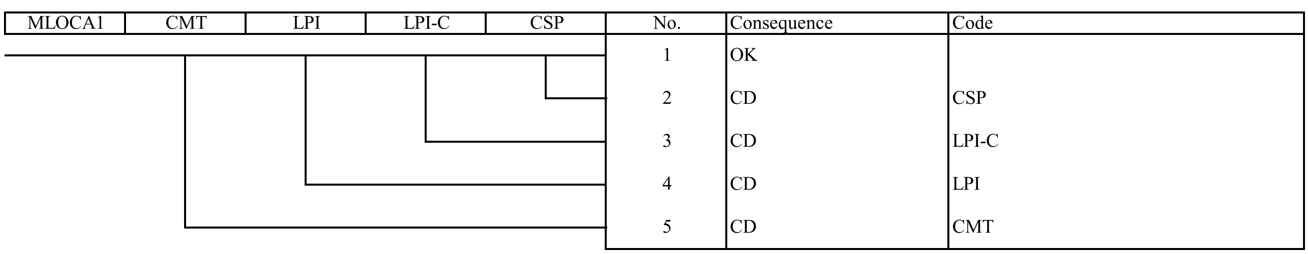

Fig. 6 FNPP event tree (secondary event: MLOCA)

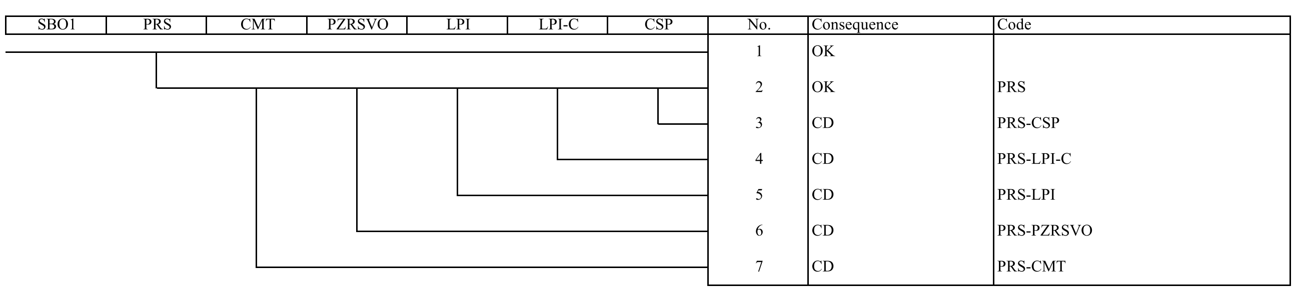

Fig. 7 FNPP event tree (secondary event: SBO)

Fig. 8 FNPP fault tree (function event: DGEN)

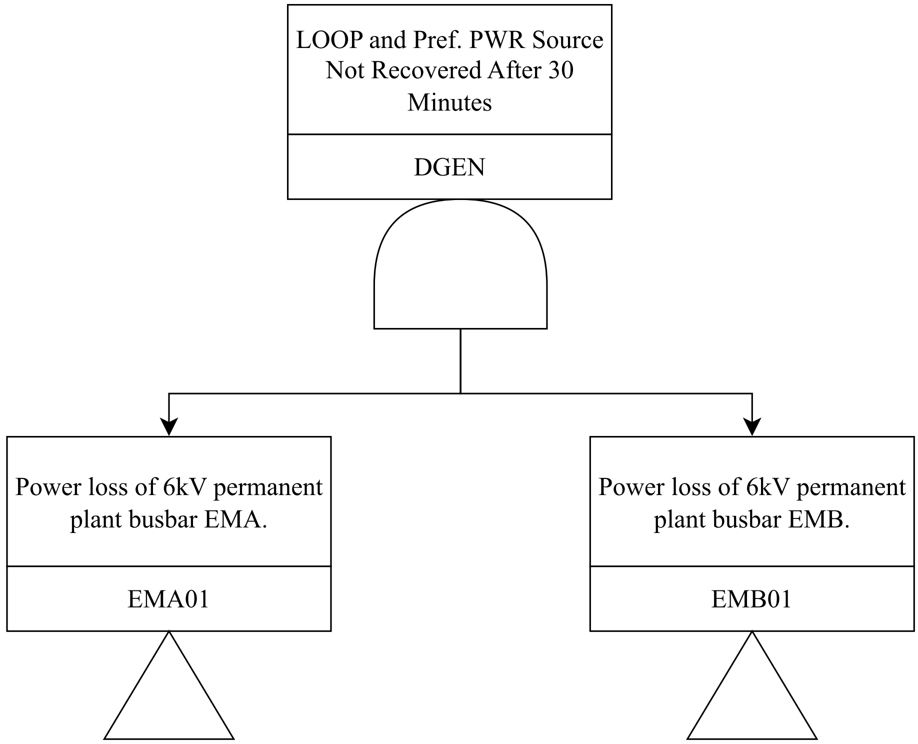

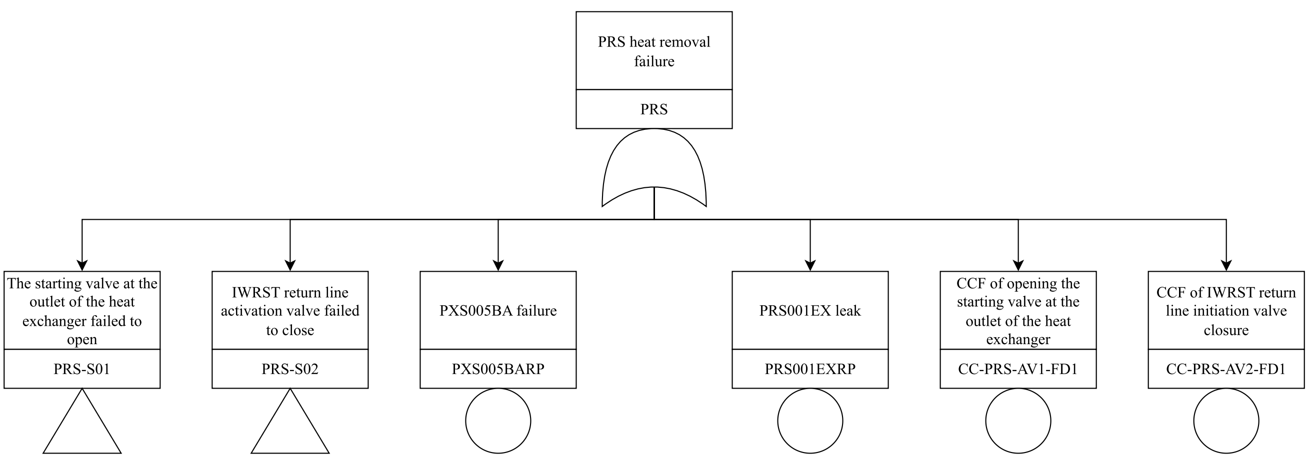

Fig. 9 FNPP fault tree (function event: PRS)

Table 6 Probability of annual excess. The confidence boundary for the parameter uncertainty is 95%

Distribution	SLR = 1.3 cm/mm	
Snow depth (Gumbel)	6.37×10^{-5}	$(3.65 \times 10^{-5}, 1.05 \times 10^{-4})$
Snow speed (Weibull)	7.85×10^{-15}	$(2.63 \times 10^{-18}, 5.78 \times 10^{-12})$
Distribution	SLR = 2.0 cm/mm	
Snow depth (Gumbel)	3.00×10^{-3}	$(2.08 \times 10^{-3}, 4.03 \times 10^{-3})$
Snow speed (Weibull)	2.24×10^{-8}	$(8.43 \times 10^{-10}, 3.95 \times 10^{-7})$

(8.5×10^{-4}). This result is similar to the value obtained by Islam et al. using a human error assessment and reduction technique (HEART) method. In their study, the probability of personnel error in cleaning the air filter for the maintenance of a sub-item of marine engine exhaust turbochargers was 1.16×10^{-4}, which was at task Level H. Considering the similarity between these two tasks and the increasing difficulty of the task under extreme snowfall conditions, if the task was assigned to Level G, the probability of personnel error obtained by using the HEART method during the snow removal process was 5.8×10^{-4}.

The probability of failure of a person receiving good training to perform the step-by-step task under a high-pressure level was used to estimate P_{RM} (6.5×10^{-3}). This result is similar to that of Shufan Li [41] regarding the personnel unreliability during small LOCA of FNPPs. (The probability of human failure is 5.8×10^{-3}.)

For simplification, we used the values of NUREG/CR-1278 to consider the personnel errors during the snow removal process. The aforementioned parameter uncertainty was considered to obey a Lognormal distribution, and the error factor (EF) was conservatively considered as $EF = 30$.

5 Result and analysis

5.1 Event sequences and MCS

We used a Risk Spectrum software to analyze the constructed model. Our calculated CDF for extreme snow was 1.13×10^{-10}/plant year, with a 95% upper limit of 4.18×10^{-10}/plant year and a 5% upper limit of 3.34×10^{-13} /plant year. Compared to the total CDF of the Level 1 PSA of the IEs for operations at ACP100 (approximately 1.42×10^{-7} /reactor year [4, 35]), extreme snowfall was determined to be three to four orders of magnitude lower, indicating that the risk caused by extreme snowfall is relatively small. As shown in Tables 7 and 8, the primary sequence of events leading to extreme snow CD is as follows:

- After extreme snowfall, the CMT and PRS fail.
- After extreme snowfall, the opened pressurizer safety valve fails to close (PZRSVC), PRS fails, and the low-pressure safety injection fails.
- After extreme snowfall, snowfall removal fails, PRS fails, and the low-pressure safety injection fails.

The results of the cut-set analysis indicate that the CCFs of the IRWST pipeline, the outlet pneumatic valve of the heat exchanger, and CCFs of the check valve are the main reasons leading to core damage owing to the extreme snow. We

Table 7 Dominant MCS

No	CDF/plant year	Proportion (%)	Minimum cut-set
1	1.78×10^{-11}	15.69	SNOW CC-CMT-AV1-FD1 CC-PRS-AV1-FD1
2	1.78×10^{-11}	15.69	SNOW CC-CMT-AV1-FD1 CC-PRS-AV2-FD1
3	1.46×10^{-11}	12.9	SNOW CC-CMT-CV-RP CC-PRS-AV1-FD1
4	1.46×10^{-11}	12.9	SNOW CC-CMT-CV-RP CC-PRS-AV2-FD1
5	1.15×10^{-12}	1.02	SNOW CC-LPI-MV-FD2 CC-PRS-AV2-FD1 SWR

recommend increasing staff awareness regarding extreme snowfalls and the reliability of snow removal, as well as improving the monitoring of critical components such as the valves and equipment vents.

5.2 Sensitivity analysis

First, we conducted a sensitivity analysis of the frequency of the initiating events. We assumed that snow depths of 50 cm and 150 cm can lead to LOOP and used the corresponding annual exceedance frequencies of 9.87×10^{-2} and 8.37×10^{-5} as the initiating frequencies of the event. Correspondingly, the CDF changed from 1.13×10^{-10} to 3.72×10^{-9} and 3.15×10^{-12}, respectively. This result was significantly smaller than the CDF obtained from the Level 1 PSA analysis of the internal event.

Meteorological departments can use weather forecasts to predict the occurrence of snowfall, personnel reliability can be significantly improved, and staff can effectively remove snow to avoid clogging the ventilation vents, to improve power availability. Assuming that the staff successfully removed the snow, a new CDF of 1.01×10^{-10} was obtained. The CDF has decreased by approximately 10%.

6 Conclusion

A methodological study for the probabilistic safety analysis of external events caused by extreme snowfall in floating nuclear power plants was presented. The

Table 8 MCS description

MCS Code	Description
CC-CMT-AV1-FD1	CCF of CMT pneumatic valve opening
CC-PRS-AV1-FD1	CCF of PRS pneumatic valve opening at the outlet of heat exchanger
CC-PRS-AV2-FD1	CCF of IRWST line pneumatic valve opening
CC-CMT-CV-RP	CCF of four normally open check valves in CMT 2 trains
CC-LPI-MV-FD2	CCF of electric valve opening in gravity injection pipeline

Table 9 Lookup table of $D(n, \alpha)$

n	Significance level α					
	0.40	0.20	0.10	0.05	0.04	0.01
5	0.369	0.447	0.509	0.562	0.580	0.667
10	0.268	0.322	0.368	0.409	0.422	0.487
20	0.192	0.232	0.264	0.294	0.304	0.352
30	0.158	0.190	0.217	0.242	0.250	0.290
50	0.123	0.149	0.169	0.189	0.194	0.225
> 50	$\frac{0.87}{\sqrt{n}}$	$\frac{1.07}{\sqrt{n}}$	$\frac{1.22}{\sqrt{n}}$	$\frac{1.36}{\sqrt{n}}$	$\frac{1.37}{\sqrt{n}}$	$\frac{1.63}{\sqrt{n}}$

primary conclusions of the analysis are as follows: (1) The intensity of the extreme snowfall specific to the plant site can be characterized by the snow depth and rate of snowfall. The use of the Gumbel and Weibull distributions to fit the annual exceedance probability of the snow thickness and snowfall rate demonstrates good applicability. (2) The significant impacts of extreme snowfall on floating nuclear power plants include the loss of off-site power and unavailability of diesel generators owing to snow blockage at the air vents; extreme snowfall presents challenges for the pneumatic and check valves in related safety systems. (3) The PSA of extreme snowfall for a specific floating nuclear power plant can be conducted based on a Level 1 PSA of an internal event. The results of the quantitative analysis demonstrate that the CDF of extreme snow is 1.13×10^{-10}.

In addition, note that the quantitative calculation of CDF is based on analyzing the extreme snow hazards. We adopted conservative assumptions and were aware of the uncertainties in meteorological data that can lead to uncertainties in the frequency of the initiating events that span several orders of magnitude, which can be compensated for by a more detailed meteorological data collection and hazard analysis.

Appendix A: K-S test

When the distribution of population X is unknown, hypothesis testing of the population distribution (goodness-of-fit test) can be performed using the Kolmogorov–Smirnov (K-S) test on samples from the population. The main steps involved are as follows:

1. Hypothesis formulation H_0: A hypothesis H_0 regarding the population distribution is proposed, typically specifying the distribution type and relevant parameters. The cumulative distribution function of the population X is $F(x;\theta_1, ..., \theta_m)$.
2. Sample data (with a sample size of n) are used to estimate the distribution parameters $(\theta_1, ..., \theta_m)$ through fitting methods such as least squares, maximum likelihood, and method of moments.
3. The value range of X is divided into k groups $[x_{i-1}, x_i](i = 1, ..., k)$.
4. A cumulative distribution function of the sample observations is calculated $F_n(x) = n_x/n$, where n_x represents the number of samples equal to or less than x.
5. Test statistics are built: $D_n = \max |F(x) - F_n(x)|$.
6. Based on the sample size n and significance level α, the critical value $D(n, \alpha)$ is obtained through a table lookup (see Table 9), and a rejection domain $D_n > D(n, \alpha)$ is constructed.
7. If the test statistic falls into the rejection domain, the hypothesis H_0 is rejected; otherwise, there is no sufficient reason to reject H_0 based on the current sample.

Acknowledgements This study received no specific grants from funding agencies in the public, commercial, or non-profit sectors.

Author contributions All authors contributed to the study conception and design. Material preparation, data collection, and analysis were performed by Lan-Xin Gong and Qing-Zhu Liang. The supervision and review of the manuscript were performed by Chang-Hong Peng. The first draft of the manuscript was written by Lan-Xin Gong, and all authors commented on previous versions of the manuscript. All authors read and approved the final manuscript.

Data availability The data that support the findings of this study are openly available in Science Data Bank at https://doi.org/10.57760/sciencedb.12003 and https://cstr.cn/31253.11.sciencedb.12003.

Declarations

Conflict of interest The authors declare that they have no competing interests.

References

1. Q. Li, D.R. Song, W. Zeng et al., Overall design and verification of ACP100S floating nuclear power plant. Nucl. Power Eng. **41**(05), 189–192 (2020). https://doi.org/10.13832/j.jnpe.2020.05.0189. (**in Chinese**)
2. D.R. Song, Q. Li, D. Qin et al., Key technology of ACP100: reactor core and safety design. Nucl. Power Eng. **42**(4), 1–5 (2020). https://doi.org/10.13832/j.jnpe.2021.04.0001. (**in Chinese**)
3. D.H. Wang, Q. Li, D.R. Song et al., Overall study of dock-based floating nuclear power plant. Nucl. Power Eng. **44**, 1–8 (2023). https://doi.org/10.13832/j.jnpe.2023.04.0001. (**in Chinese**)
4. J. Deng, Y.Y. Xu, Z.F. Qiu et al., Research on level 1 PSA and risk-informed design for ACP100. Ann. Nucl. Energy **144**, 107542 (2020). https://doi.org/10.1016/j.anucene.2020.107542
5. X. Jie, Research progress of reactor thermal-hydraulic characteristics under ocean conditions in China. Front. Energy Res. **8**, 593362 (2020). https://doi.org/10.3389/fenrg.2020.593362
6. J.Y. Li, D.H. Wang, M. Zhang, et al., Study of stress analysis method for floating nuclear power plant containment under combined multiple loads. in *Paper presented at Proceedings of the 23rd Pacific Basin Nuclear Conference*, Chengdu, China, Oct 31st to Nov 4, (2022). https://doi.org/10.1007/978-981-99-1023-6_69
7. J. Qiu, L. Li, Y. Tai et al., MELCOR simulation of the SBLOCA induced severe accident for the SMR in a floating nuclear power plant. Prog. Nucl. Energy **129**, 103509 (2020). https://doi.org/10.1016/j.pnucene.2020.103509
8. J.X. Xiao, X.Y. Xu, H. Zhang et al., A method for hazard analysis of a floating nuclear power plant subjected to ship collision. Ann. Nucl. Energy **190**, 109870 (2023). https://doi.org/10.1016/j.anucene.2023.109870
9. A. Bareith, Z. Karsa, T. Siklossy, et al., External events PSA for the paks NPP (NEA-CSNI-R–2014-9). PSA of natural external hazards including earthquakes. Nucl. Energy Agency of the OECD (NEA), (2014). https://inis.iaea.org/collection/NCLCollectionStore/_Public/46/027/46027285.pdf
10. American Society of Mechanical Engineers/American National Standards Institute, *Probabilistic Risk Assessment Standard for Advanced Non-Light Water Reactor Nuclear Power Plants*. (United States, 2021)
11. American Society of Mechanical Engineers/American National Standards Institute, *Standard for Level 1/Large Early Release Frequency Probabilistic Risk Assessment for Nuclear Power Plant Applications*. (United States, 2022)
12. International Atomic Energy Agency, *Site Evaluation for Nuclear Installations*. (Vienna, 2019). https://www-pub.iaea.org/MTCD/publications/PDF/P1837_web.pdf
13. International Atomic Energy Agency, *Development and Application of Level 1 Probabilistic Safety Assessment for Nuclear Power Plants*. (Vienna, 2010). https://www-pub.iaea.org/mtcd/publications/pdf/pub1430_web.pdf
14. A. Wielenberg, M. Hage, H. Loeffler, et al., Methodology for selecting initiating events and hazards for consideration in an extended PSA. (Advanced Safety Assessment Methodologies: Extended PSA Web, 2017), http://asampsa.eu/wp-content/uploads/2014/10/ASAMPSA_E-D30.7-vol-2-initiating-events-selection.pdf. Accessed 20 June (2023)
15. Y. Narumiya, H. Nomura, T. Nakayama, et al., A study of screening method for the risk significant combinations among the external hazards. in *Paper presented in Proceedings of the 13th International Conference on Probabilistic Safety Assessment and Management (PSAM 13)*, Seoul, Korea, (2-7 October 2016). https://iapsam.org/PSAM13/program/Abstract/Oral/A-552.pdf
16. E. Choi, J.G. Ha, D. Hahm et al., A review of multihazard risk assessment: progress, potential, and challenges in the application to nuclear power plants. Int. J. Disast. Risk Re. **53**, 101933 (2021). https://doi.org/10.1016/j.ijdrr.2020.101933
17. K. Kubo, S. Jang, T. Takata et al., Dynamic probabilistic risk assessment of seismic-induced flooding in pressurized water reactor by seismic, flooding, and thermal-hydraulics simulations. J. Nucl. Sci. Technol. **60**, 359–373 (2022). https://doi.org/10.1080/00223131.2022.2100837
18. H. Yamano, H. Nishino, K. Kurisaka, Development of probabilistic risk assessment methodology of decay heat removal function against combination hazards of strong wind and rainfall for sodium-cooled fast reactors. in *Paper presented at Proceedings of the 25th International Conference on Nuclear Engineering, Shanghai, China*, (2-6 July 2017). https://doi.org/10.1115/ICONE25-66059
19. I.G. Kantarzhi, V.S. Maderich, V.I. Koshebutskii, Determination of ice characteristics for marine hydroengineering structures. Power Technol. Eng. **49**, 345–353 (2016). https://doi.org/10.1007/s10749-016-0626-6
20. H. Nishino, H. Yamano, K. Kurisaka, Development of probabilistic risk assessment methodology of decay heat removal function against combination hazard of low temperature and snow for sodium-cooled fast reactors. in *Proceedings of the 25th International Conference on Nuclear Engineering*, Shanghai, China, (2-6 July 2017). https://doi.org/10.1115/ICONE25-67627
21. H. Yamano, H. Nishino, K. Kurisaka et al., Development of probabilistic risk assessment methodology against extreme snow for sodium-cooled fast reactor. Nucl. Eng. Des. **308**, 86–95 (2016). https://doi.org/10.1016/j.nucengdes.2016.08.006
22. Z. Kovacs, External event level 1 PSA for the WWER44 type reactors in Slovakia. in *Paper presented at the International Conference on Topical Issues in Nuclear Installation Safety, Vienna, Austria, 6-9 June (2017)*. https://www-pub.iaea.org/MTCD/Publications/PDF/AdditionalVolumes/STIPUB1829_volTwoWeb.pdf
23. J. Sandberg, U. Vuorio, The role of external events PSA in the Finnish regulatory approach. (IAEA web, 2014), https://inis.iaea.org/collection/NCLCollectionStore/_Public/46/027/46027298.pdf. Accessed (20 June 2023)
24. J. Králik, Probabilistic analysis of machine tool structures fragility to extreme snow impact. in *26th International Conference on Engineering Mechanics 2020, Brno, Czech Republic*, November 24–25, (2020). https://doi.org/10.21495/5896-3-302
25. H. Yamano, H. Nishino, K. Kurisaka, et al., Development of risk assessment methodology of decay heat removal function against external hazards for sodium-cooled fast reactors: (1) Project overview and margin assessment methodology against snow. in *Paper presented at Proceedings of the 23rd International Conference on Nuclear Engineering, Makuhari, Chiba, Japan*, May 17-21, (2015). https://doi.org/10.1299/jsmeicone.2015.23._ICONE23-1_2

26. M.S. Hoseyni, K. Karimi, S.M. Hoseyni et al., Success criteria analysis in support of probabilistic risk assessment for nuclear power plants: application on SGTR accident. Nucl. Sci. Tech. **28**, 33 (2017). https://doi.org/10.1007/s41365-017-0193-z
27. J.X. Zuo, J.P. Jing, J.S. Bi et al., Framework analysis of fluoride salt-cooled high temperature reactor probabilistic safety assessment. Nucl. Sci. Tech. **26**, 050602 (2015). https://doi.org/10.13538/j.1001-8042/nst.26.050602
28. K. Tamori, T. Kyoshi, A research on optimization of plotting position. Transactions of the 2009 Japan Society of Civil Engineers **66**, B-27 (2009). 10.2208%2Fjscejf.66.112
29. A.S. Yahaya, C.S. Yee, N.A. Ramli et al., Determination of the best probability plotting position for predicting parameters of the Weibull distribution. Int. J. Appl. Sci. Technol. **2**(3), 106–111 (2012)
30. T.B. Arnold, J.W. Emerson, Nonparametric goodness-of-fit tests for discrete null distributions. R J. **2**(3), 34–39 (2011). https://doi.org/10.32614/RJ-2011-016
31. Academy of agricultural planning and engineering (MARA): National meteorological data, http://data.sheshiyuanyi.com/. Accessed 20 June 2023
32. National centers for environmental information, https://www.ncei.noaa.gov/maps/daily/. Accessed 20 June 2023
33. C.F. Yang, X.Q. Zhu, Analysis on statistical characteristics of snow-to-liquid ratio in Shandong. J. Mar. Meteorol. **40**(1), 47–56 (2020). https://doi.org/10.19513/j.cnki.issn2096-3599.2020.01.005. (**in Chinese**)
34. M. Esfandiari, G. Jahanfarnia, K. Sepanloo et al., Loss of offsite power(LOOP) accident analysis by integration of deterministic and probabilistic approaches in Bushehr-1 VVER-1000/V446 nuclear power plant. Nucl. Sci. Tech. **33**, 56 (2022). https://doi.org/10.1007/s41365-022-01044-8
35. D.R. Song, C.M. Liu, *Multi-purpose Modular Small Nuclear Reactor* (China Atomic Energy Press, Beijing, 2021). (**in Chinese**)
36. L.L. Tong, X.W. Cao, Methodology for reliability allocation based on fault tree analysis and dualistic contrast. Nucl. Sci. Tech. **19**, 251–256 (2008). https://doi.org/10.1016/S1001-8042(08)60059-7
37. R.L. Brune, M. Weinstein, M.E. Fitzwater, Peer-review study of the draft handbook for human-reliability analysis with emphasis on nuclear-power-plant applications, NUREG/CR-1278. (Human Performance Technologies Inc., Thousand Oaks, CA (USA), 1983); https://www.osti.gov/servlets/purl/6392305). Accessed 20 June (2023)
38. Z.G. Ma, T.E. Wierman, K.J. Kvarfordt, Industry-average performance for components and initiating events at U.S. commercial nuclear power plants: 2020 update. (OSTI Web, 2021), https://www.osti.gov/biblio/1847110. Accessed 20 June (2023). https://doi.org/10.2172/1847110
39. A. Noroozi, R. Abbassi, S. MacKinnon et al., Effects of cold environments on human reliability assessment in offshore oil and gas facilities. Human Factors **56**(5), 825–839 (2014). https://doi.org/10.1177/0018720813512328
40. R. Islam, R. Abbassi, V. Garaniya et al., Development of a human reliability assessment technique for the maintenance procedures of marine and offshore operations. J. Loss Prevent. Proc. **50**, 416–428 (2017). https://doi.org/10.1016/j.jlp.2017.10.015
41. S.F. Li, Research on human reliability of floating nuclear power plant based on Bayesian networks, Nanhua University, (2019). https://doi.org/10.27234/d.cnki.gnhuu.2019.000607. (**in Chinese**)